Mask free Intravenous 3D Digital Subtraction Angiography (IV 3D-DSA) from a single C-arm acquisition

Yinsheng Li[a], **Kai Niu**[a], **Pengfei Yang**[b], **Beveley Aagaard-Kienitz**[b], **David B. Niemann**[c], **Azam S. Ahmed**[c], **Charles Strother**[b], and **Guang-Hong Chen**[a,b]

[a]Department of Medical Physics, University of Wisconsin-Madison, WI 53705

[b]Department of Radiology, University of Wisconsin-Madison, WI 53792

[c]Department of Neurological Surgery,University of Wisconsin-Madison, WI, 53792

Abstract

Currently, clinical acquisition of IV 3D-DSA requires two separate scans: one mask scan without contrast medium and a filled scan with contrast injection. Having two separate scans adds radiation dose to the patient and increases the likelihood of suffering inadvertent patient motion induced mis-registration and the associated mis-registraion artifacts in IV 3D-DSA images. In this paper, a new technique, SMART-RECON is introduced to generate IV 3D-DSA images from a single Cone Beam CT (CBCT) acquisition to eliminate the mask scan. Potential benefits of eliminating mask scan would be: (1) both radiation dose and scan time can be reduced by a factor of 2; (2) intra-sweep motion can be eliminated; (3) inter-sweep motion can be mitigated. Numerical simulations were used to validate the algorithm in terms of contrast recoverability and the ability to mitigate limited view artifacts.

Keywords

Digital Subtraction Angiography (DSA); Single C-arm acquisition; C-arm Cone Beam Computer Tomography (CBCT); Temporal Resolution Improvement

1. INTRODUCTION

Cerebral aneurysm is a weak or thin spot on a cerebral blood vessel that fills with blood and balloons out. It can press on a nerve or surrounding tissues and can leak or burst, which may induces hemorrhage. Treatment is necessary to prevent the aneurysm from rupturing. It can be done by placing a metal clip at the base of the aneurysm or by inserting metal coils that induce clot formation within the aneurysm. Conventional two dimensional Digital Subtraction Angiography (2D-DSA) has been widely used in early diagnosis and prognosis of cerebral aneurysm.[1–3] The 3D-DSA improves aneurysm detection and delineation with lower radiation dose, less contrast use, and shorter procedural time compared to 2D-DSA.[4,5]

Three-dimensional digital subtraction angiography (3D-DSA) with intravenous contrast injection (IV 3D-DSA) plays an increasingly important role in the diagnosis and treatment of aneurysms. Currently, the acquisition of IV 3D-DSA requires two separate scans: a mask scan without contrast and a filled scan with contrast. In clinical practice, the added radiation

dose and misregistration artifacts due to patient inter-scan motion are two major concerns of IV 3D-DSA which limit its clinical utility. To improve IV 3D-DSA image quality and to address the potential radiation concerns, these two challenges will need to be addressed simultaneously.

The purpose of this work is to generate IV 3D-DSA image volumes from a single sweep C-arm data acquisition. To achieve this goal, two or more entire Field-of-View (FOV) image volumes must be reconstructed from the single sweep dataset, and these image volumes must have significant contrast differences in order to perform subtraction for the generation of 3D-DSA images. In a single sweep C-arm CBCT acquisition within short scan angular range of about $200°$, the data is only sufficient for the reconstruction of one temporally averaged image using the conventional Filtered Back Projection (FBP) reconstruction method. Attempts to reconstruct two or more image volumes result in devastating limited view angle artifacts. Although iterative reconstruction algorithms such as Prior Image Constrained Compressed Sensing (PICCS)[6,7] were introduced to iteratively reconstruct two image volumes from one short scan data set, the contrast difference in these two image volumes may not be sufficient to generate the desired subtracted angiograms even if the contrast injection protocol used clinically is able to capture the entire contrast agent wash-in and wash-out curve within the single sweep C-arm acquisition.

In this work, a new reconstruction method was used to generate three image volumes from one short scan range. These three image volumes can have significantly different contrast enhancement and thus a subtraction between the two image volumes with the largest difference enables us to generate the desired IV 3D DSA angiograms. The technical foundation of this work is our recently published iterative image reconstruction algorithm: Synchronized MultiArtifact Reduction with Tomographic reconstruction (SMART-RECON).[8] Numerical simulations were used to validate the algorithm in terms of contrast recoverability and the ability to mitigate artifacts.

2. METHODS AND MATERIALS

2.1 SMART-RECON framework

Unlike other well known iterative reconstruction methods, SMART-RECON primarily exploits the intrinsic low dimensionality of the spatial-temporal image matrix to regularize the reconstruction. Namely, it can be formulated as the following convex optimization problem:

$$\tilde{\mathbf{X}} = \underset{\mathbf{X}}{arg\min} \frac{1}{2}\left(\overrightarrow{\mathscr{Y}} - \mathscr{A}\overrightarrow{\mathbf{X}}\right)^{tr} \mathrm{D} \left(\overrightarrow{\mathscr{Y}} - \mathscr{A}\overrightarrow{\mathbf{X}}\right) + \lambda\|\mathbf{X}_A\|_* \quad (1)$$

where $\overrightarrow{\mathscr{Y}}$ is the vectorized projection data and $\overrightarrow{\mathbf{X}}$ is the vectorized spatial-temporal image matrix. The prior image column vector, $\overrightarrow{X}^p$, is used to augment the target spatial-temporal image matrix $\mathbf{X}$ to generate the augmented spatial-temporal matrix $\mathbf{X}_A$. The diagonal matrix D has the inverse of the noise variance of the log-transformed data as its diagonal elements. The notation $(\cdot)^{tr}$ is the transpose operator. The parameter λ is introduced to control the

balance between the data fidelity term and the regularizer strength. The nuclear norm of this latter matrix, i.e., $\|\mathbf{X}_A\|_*$, is used to regularize the reconstruction of the spatial-temporal matrix, $\mathbf{X}$.

$$\mathbf{X}_A = (\overrightarrow{X}^p | \mathbf{X}) =: \begin{pmatrix} X_1^p & X_1^1 & X_1^2 & \cdots & X_1^T \\ X_2^p & X_2^1 & X_2^2 & \cdots & X_2^T \\ \vdots & \vdots & \vdots & \ddots & \vdots \\ X_M^p & X_M^1 & X_M^2 & \cdots & X_M^T \end{pmatrix} \tag{2}$$

where =: stands for a definition. The nuclear norm of this matrix, i.e., $\|\mathbf{X}_A\|_*$, is used to regularize the reconstruction of the spatial-temporal matrix, $\mathbf{X}$. Namely, the regularizer is given as below:

$$\|\mathbf{X}_A\|_* = \|\mathbf{U}\sum\mathbf{V}^{tr}\|_* \sum_r \sigma_r \tag{3}$$

where $\mathbf{X}_A = \mathbf{U}\mathbf{\Sigma}\mathbf{V}^{tr}$ is the singular value decomposition (SVD) of the matrix $\mathbf{X}_A$. In this decomposition $\mathbf{U}$ and $\mathbf{V}$ are two orthogonal matrices, and $\mathbf{\Sigma} = diag\{\sigma_r\}$ is a diagonal matrix. The values σ_r ($r = 1, 2, \ldots$) are also known as the singular values of the prior image augmented spatial-temporal image matrix $\mathbf{X}_A$. In this work, the FBP reconstruction from all available time-frames was used to generate the prior image. Projection data from the entire short scan range was separated into 3 or 4 subsets corresponding to narrower angular spans.

Each subset of the projection data forms the vector $\overrightarrow{\mathcal{Y}}$. Each reconstructed image volume corresponding to one subset forms the spatial-temporal image matrix $\mathbf{X}$.

The above convex optimization problem 1 can be solved using the recently developed alternated updating method[9] to decompose the original optimization problem into two sub-problems,

$$\overrightarrow{\mathbf{X}}^{(k)} = arg \min_{\overrightarrow{\mathbf{x}}} \frac{1}{2}\left(\overrightarrow{\mathcal{Y}} - \mathscr{A}\overrightarrow{\mathbf{X}}\right)^{tr} \mathrm{D}\left(\overrightarrow{\mathcal{Y}} - \mathscr{A}\overrightarrow{\mathbf{X}}\right) \tag{4}$$

$$\mathbf{X}_A^{(k+1)} = arg \min_{\mathbf{X}_A} \frac{1}{2}\|\mathbf{X}_A - \mathbf{X}_A^{(k)}\|_F^2 + \lambda\|\mathbf{X}_A\|_* \tag{5}$$

where $\|\mathbf{X}\|_F^2 =: \sum_{ij} X_{ij}^2$ is the Frobenius norm of the real matrix $\mathbf{X}$. The quadratic problem in Eq. (4) can be easily solved iteratively using the following update sequence:

$$\overrightarrow{\mathbf{X}}^{(k)} = \overrightarrow{\mathbf{X}}^{(k-1)} + \delta\mathscr{A}^{tr}\mathrm{D}\left[\overrightarrow{\mathcal{Y}} - \mathscr{A}\overrightarrow{\mathbf{X}}^{(k-1)}\right] \tag{6}$$

After the k-th iteration of the image column vector $\vec{\mathbf{X}}$, i.e., $\vec{\mathbf{X}}^{(k)}$, is computed using the above formula, it is converted back to its spatial-temporal matrix form $\mathbf{X}^{(k)}$. The parameter δ is the updating step size. It was emperically fixed to 0.25 in this study. The modified denoising problem in Eq. (5) is then solved to obtain the denoised spatial-temporal matrix denoted by $\mathbf{X}^{(k+1)}$:

$$\mathbf{X}_A^{(k+1)} = SVT_\lambda(\mathbf{X}_A^{(k)}) \quad (7)$$

where the singular value thresholding (SVT) function $SVT_\lambda(\mathbf{X})$ is defined as follows,[10]

$$SVT_\lambda(\mathbf{X}) = \boldsymbol{U}\left(\sum - \lambda \boldsymbol{I}\right)_+ \boldsymbol{V}^{tr} \quad (8)$$

$$\left(\sum - \lambda \mathbf{I}\right)_+ = \begin{cases} \sigma_i - \lambda, & \sigma_i \geq \lambda \\ 0, & \sigma_i < \lambda \end{cases} \quad (9)$$

where $\mathbf{I}$ is an identity matrix. This two-step optimization strategy has been proven to be linearly convergent.[9] The implementation details can be referred to in Chen and Li.[8,9,11]

2.2 Simulated phantom study

In numerical simulations, a sequence of time-resolved human cerebral angiograms with a peak iodinated contrast enhancement of 400 HU was used to generate synthesized fan-beam projection data by a forward projection procedure. The peak enhancement was similar to a CT angiography acquisition at 80 kVp using an intravenous contrast injection protocol and a 350 mg I/ml contrast solution. The projection data was simulated without noise. The total view angle span in the numerical simulations was restricted to the short scan angular span of $240\,^\circ$ with a $60\,^\circ$ fan angle. An image matrix size of 320×320, corresponding to a 0.5 mm^2 pixel size, was used for image reconstruction. 656 view angles were acquired over the short scan angular span with 888 detector elements across the entire scanning field of view.

For quantitative comparison, the the relative root mean square error (rRMSE) was calculated for the short scan FBP reconstruction result (where only a single image can be reconstructed), and for the SMART-RECON images at each of the four time frames. The rRMSE for an image x is defined as

$$rRMSE(x) = \frac{\sqrt{\sum_i \left(x_i - x_i^{\text{truth}}\right)^2}}{\sum_i \left|x_i^{\text{truth}}\right|} \times 100\% \quad (10)$$

where x^{truth} is the ground truth reference image, and the subscript i denotes the pixel location in the image.

3. RESULTS

Numerical simulation results are presented in Figure 1. The first row shows the reference images for each time frame. The second and third rows show the corresponding time frames reconstructed with FBP and SMART-RECON methods, respectively. The reference images were reconstructed using FBP from projection data covering the entire short scan angular span for each of the individual image time frames. One may observe in Figure 1, SMART-RECON enables a clear reconstruction of arteries and veins with good quality for all four time frames. The rRMSEs were calculated for the respective time frames reconstructed with FBP and SMART-RECON to provide an overall quantification of reconstruction accuracy and it is shown in Figure 2.

4. DISCUSSIONS AND CONCLUSIONS

In this work, IV 3D-DSA angiograms can be generated from a single C-arm cone beam CT acquisition to reduce radiation dose by a factor of two, to reduce scanning time by a factor of 2, to eliminate inter-sweep motion induced by patient and to reduce the intra-sweep motion. Images reconstructed from SMART-RECON show improved visualization of vessels.

The technical challenge of single acquisition 3D-DSA is to reconstruct at least two image volumes with contrast variation from the short scan angular data. To reconstruct a image volume using the data angular range narrower than short scan range using FBP, severe limited view artifacts make images useless. A recently proposed algorithm SMART-RECON can be used to mitigate temporal averaged artifacts and eliminate limited view artifacts simultaneously. To eliminate limited-view artifacts, two things are special in SMART-RECON: (1) the nuclear norm of the spatial-temporal matrix is used to promote similarity between different image columns and thus to mitigate limited view artifacts; (2) a limited-view artifacts free prior image is used to augment the spatial-temporal matrix to further sparsify images and to reduce limited view artifacts.

Algorithm is operated in a local workstation equipped with an nVidia GTX Titan Z GPU (nVidia, Santa Clara, CA). It takes 30s to complete one iteration. Normally, 15 iterations are sufficient to achieve the empirical convergence.

Clinical validation using animal data and human subject data would be our future works. Using animal experiments, contrast agent injection protocol can be optimized for SMART-RECON. Basically, one of the scientific question that is needed to be addressed is to determine the optimal contrast bolus delay time for both FBP reconstruction and SMART-RECON algorithm.

Acknowledgments

References

1. Brody WR. Digital subtraction angiography. Nuclear Science, IEEE Transactions on. 1982; 29(3): 1176–1180.

2. Meaney, TF., Weinstein, M., Buonocore, E., Pavlicek, W., Borkowski, GP., Gallagher, JH., Sufka, B., Maclntyre, WJ. Application of Optical Instrumentation in Medicine VIII. International Society for Optics and Photonics; 1980. Digital subtraction angiography of the human cardiovascular system; p. 272-278.

3. Chappell ET, Moure FC, Good MC. Comparison of computed tomographic angiography with digital subtraction angiography in the diagnosis of cerebral aneurysms: a meta-analysis. Neurosurgery. 2003; 52(3):624–631. [PubMed: 12590688]

4. Anxionnat R, Bracard S, Ducrocq X, Trousset Y, Launay L, Kerrien E, Braun M, Vaillant R, Scomazzoni F, Lebedinsky A, et al. Intracranial aneurysms: Clinical value of 3d digital subtraction angiography in the therapeutic decision and endovascular treatment 1. Radiology. 2001; 218(3): 799–808. [PubMed: 11230659]

5. Wong SC, Nawawi O, Ramli N, Kadir KAA. Benefits of 3d rotational dsa compared with 2d dsa in the evaluation of intracranial aneurysm. Academic radiology. 2012; 19(6):701–707. [PubMed: 22578227]

6. Chen G, Tang J, Leng S. Prior image constrained compressed sensing (PICCS): a method to accurately reconstruct dynamic CT images from highly undersampled projection data sets. Medical physics. 2008; 35:660. [PubMed: 18383687]

7. Chen G-H, Tang J, Hsieh J. Temporal resolution improvement using PICCS in MDCT cardiac imaging. Medical physics. 2009; 36(6):2130–2135. [PubMed: 19610302]

8. Chen G-H, Li Y. Synchronized multiartifact reduction with tomographic reconstruction (SMART-RECON): A statistical model based iterative image reconstruction method to eliminate limited-view artifacts and to mitigate the temporal-average artifacts in time-resolved CT. 42(8):4698–4707.

9. Li, Y., Niu, K., Tang, J., Chen, G. Proceedings of SPIE Medical Imaging. International Society for Optics and Photonics; 2014. Statistical Image Reconstruction via Denoised Ordered-Subset Statistically Penalized Algebraic Reconstruction Technique (DOS-SPART); p. 90330U-90330U.

10. Cai J-F, Candès EJ, Shen Z. A singular value thresholding algorithm for matrix completion. SIAM Journal on Optimization. 2010; 20(4):1956–1982.

11. Li, Y., Niu, K., Chen, G-H. SPIE Medical Imaging. International Society for Optics and Photonics; Statistical model based iterative reconstruction in myocardial CT perfusion: exploitation of the low dimensionality of the spatial-temporal image matrix; p. 94123N-94123N.
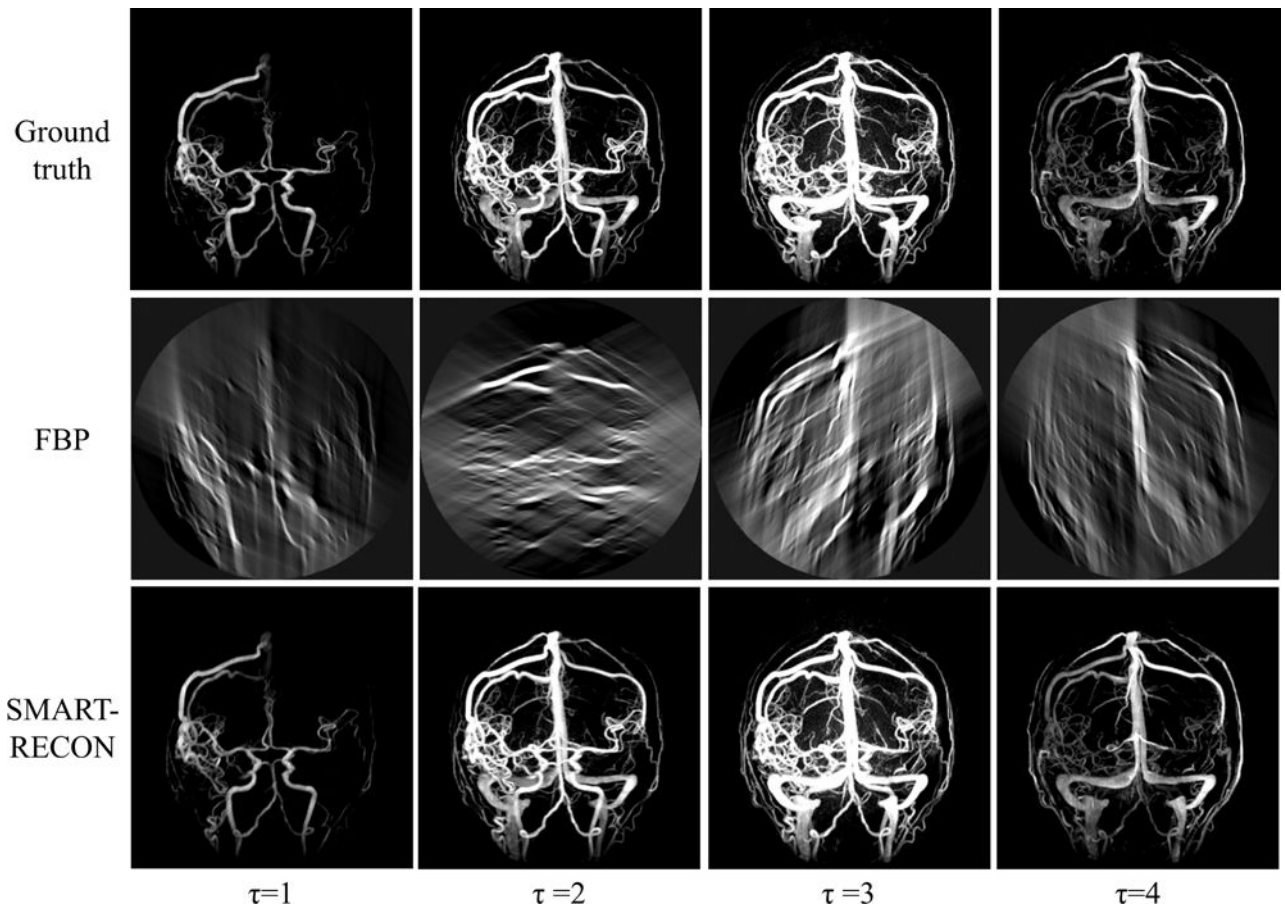
Figure 1.
Image results for four time frames for the numerical simulation studies. All images are shown with a W/L: 2000/100.
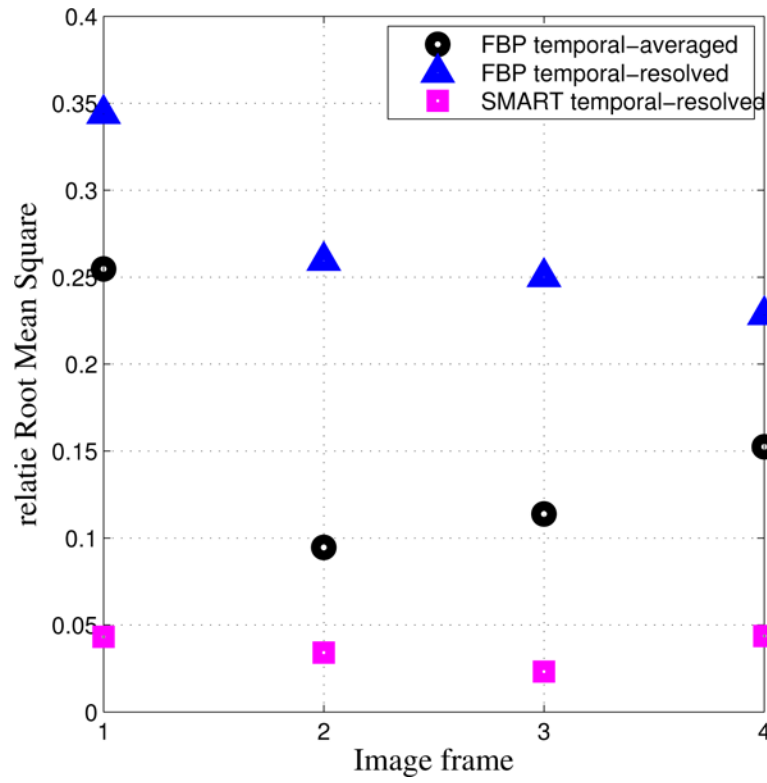
Figure 2.
Quantitative comparison between temporal averaged FBP images, FBP reconstructed images for each segment, and SMART-RECON images for each segment.